

## Ballooning, Burst and Oxidation behavior of Cr-coated ATF cladding during LOCA

Hyunwoo Yook<sup>a</sup>, SungHoon Joung<sup>a</sup>, Youho Lee<sup>a\*</sup>

<sup>a</sup>Seoul National University, 1 Gwanak-ro, Gwanak-gu, Seoul 08826, Republic of Korea

\*Corresponding author: leeyouho@snu.ac.kr

\***Keywords** : Loss Of Coolant Accident, cladding ballooning & burst, Cr-coated cladding, Accident Tolerant Fuel

### 1. Introduction

The enhanced outer wall oxidation resistance of chromium-coated Accident Tolerant Fuel (ATF) cladding is anticipated to increase the current nuclear fuel discharge burnup limit (62 GWD/MTU) by extending pressurized water reactor cycle lengths to 24 months [1], while also preserving cladding ductility by minimizing oxidation during accident scenarios. However, the significant ballooning & burst size of high burnup nuclear fuel [2], the loss of oxidation protection due to coating cracking induced by extensive deformation during Loss of Coolant Accident (LOCA), and post-burst oxidation of the inner cladding wall [3] represent primary mechanisms of cladding embrittlement that may diminish the accident tolerance of Cr-coated cladding. To implement Cr-coated cladding in commercial nuclear power plants, safety regulations and analyses considering these embrittlement behaviors are imperative, alongside the need for pertinent experimental investigations.

This study aimed to simulate Cr-coated cladding burst and double-sided oxidation during LOCA situation, and to analyze the oxidation characteristics of Cr-coated cladding with coating cracks. Burst experiments were conducted on Cr-coated cladding under various internal rod pressure conditions using LOCA facility (*i*-LOCA) at Seoul National University. The burst strain was measured under different internal pressure conditions, and observations were made of cracks in the chromium coating around the burst. Subsequently, a double-sided oxidation experiment was performed on the burst specimens to analyze the impact of coating cracking on the oxidation of Cr-coated cladding.

### 2. Experiments

Figure 1 shows the experimental procedure conducted in this study to simulate the ballooning, burst, and oxidation of Cr-coated cladding in LOCA situation. For the simulated LOCA experiment, Zr-1.1Nb cladding coated with a thickness of 16  $\mu\text{m}$  using the arc ion plating method was utilized. Cladding burst experiments, excluding oxidation, were carried out using the facility (*i*-LOCA) depicted in Figure 2(a) [4], pressurizing the cladding within the range of 1-5 MPa and elevating the temperature through induction heating within an Ar gas environment. Cylindrical ( $D=8.192\text{mm}$ ) and spherical

powder-type ( $D=0.5\text{mm}$ )  $\text{ZrO}_2$  pellets were inserted into the rod, and the cold void volume of the rod was set to 30  $\text{cm}^3$  for the burst test. The shape of the cladding burst and any coating cracks on the specimen were measured using a 3D scanner. Subsequently, the burst specimen was sectioned to 4 cm and subjected to double-sided oxidation at 1200°C for 600 seconds using the equipment depicted in Figure 2(b) [5]. Specimens that did not experience burst were also subjected to oxidation for comparison with burst specimens. The cladding weight gain during high-temperature oxidation was analyzed in relation to the shape of the cladding burst and coating cracks.



Fig. 1. Experimental procedure of this study

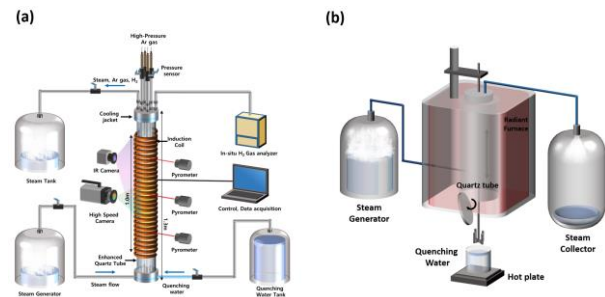


Fig. 2. Schematic diagram of two LOCA facility for (a) cladding burst [4] and (b) high temperature steam oxidation [5] in Seoul National University

### 3. Results and Discussion

Figure 3 shows the cladding ballooning, burst and fuel dispersal behavior for specimens with cylinder and powder pellet inserted. The initial internal pressure of specimens was 1 MPa, and cold void volume was controlled to 30  $\text{cm}^3$ . Larger cladding deformation with powder pellet is shown in Fig.3, indicating the cladding temperature distribution difference induced by different pellet-cladding contact. Small size of powder pellet result in the more uniform pellet-cladding contact and thereby the circumferential cladding temperature. Fuel dispersal was observed for powder pellet, simulating the fuel dispersal of high burnup fragmented fuel.

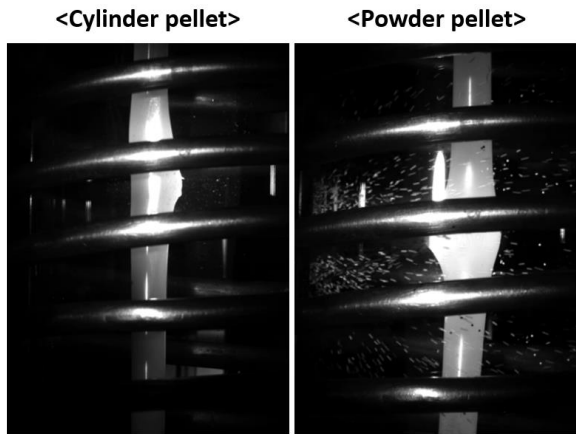


Fig. 3. Cladding ballooning, burst, and fuel dispersal behavior for specimens with cylinder and powder pellet

In Figure 4(a), the 3D measurement of a burst specimen with a circumferential strain of 25.1% is shown. The ballooning region, characterized by over 5% hoop strain, is highlighted in red, where coating cracks were observed. Figure 4(b) shows the burst circumferential strain of the specimens. The burst circumferential strain decreased with the rod initial internal pressure.

Figure 5 shows the change in the area of the inner and outer walls of a 4cm cladding tube according to the burst circumferential strain. The outer wall area was determined through the three-dimensional shape measurement results of the specimen, while the cladding thickness and inner wall area were derived from the outer wall diameter [6]. As the burst circumferential strain increased, both the inner and outer wall areas expanded. Additionally, the difference in area between the inner and outer walls decreased due to the reduced cladding thickness in the burst region.

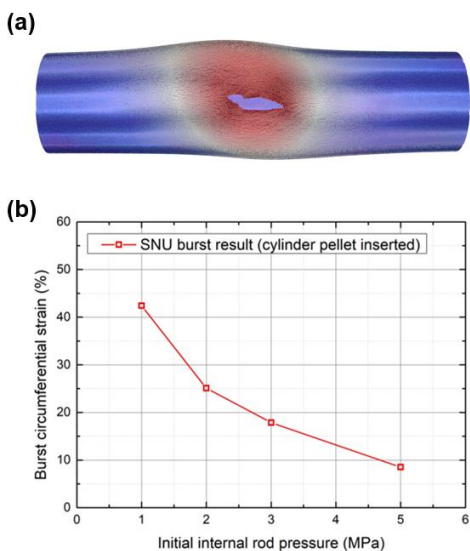


Fig. 4. (a) Burst region (>5% hoop strain) measured with 3D scanner (b) burst circumferential strain with initial internal rod pressure

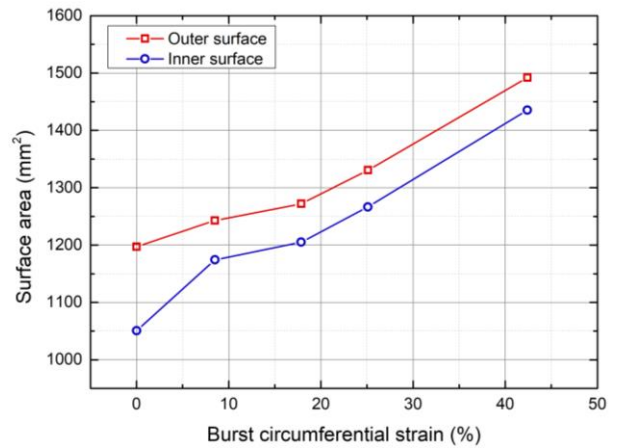


Fig. 5. Burst circumferential strain with initial rod pressure

Figure 6 shows the morphology of the coating cracks and the results of surface roughness measurements conducted on the burst specimen. With a burst circumferential strain of 25.1%, coating cracks were predominantly clustered around the burst area where the circumferential strain was elevated. Notably, in the burst region, the zircaloy surface was exposed through these cracks, as evidenced by the observable color difference in Figure 6. Furthermore, the surface roughness measurement results also confirmed the presence of coating cracks. It was observed that the crack area expanded as the circumferential strain increased when comparing burst specimens.

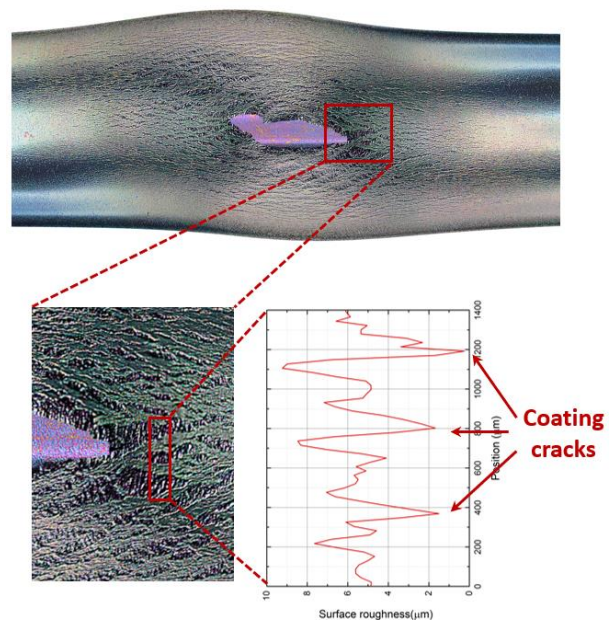


Fig. 6. Coating cracks and surface roughness in burst specimen (circumferential strain 25.1%)

Figure 7 shows the oxidation results of both burst specimens and reference non-burst specimens. In Figure 7(a), the total weight gain of the specimens is presented,

while Figure 7(b) shows the weight gain divided by the cladding surface area.

For the non-burst specimens, the average weight gain was measured and calculated to serve as a reference for the inner wall oxidation of Cr-coated cladding. Conversely, for burst specimens, the weight gain per area was determined by dividing the total weight gain by the inner and outer wall area in Fig. 5.

Comparatively, burst specimens exhibited greater oxidation compared to non-burst specimens, as evidenced by their higher total weight gain, which escalated with burst circumferential strain (Fig. 7(a)). This increased oxidation can be attributed to the expanded cladding surface area and the exposure of the zircaloy surface through cracks. Weight gain per area analysis negates the influence of increased weight gain resulting from the expanded inner and outer wall area of burst specimens, thereby highlighting the weight gain attributable to the oxidation of the zircaloy matrix exposed due to coating cracks (Fig. 7(b)).

Up to a burst circumferential strain of 25.1%, no discernible difference in weight gain was observed compared to the reference non-burst specimens. These findings indicate that although coating cracks were detected in the specimen with a circumferential strain of 25.1% as shown in Figure 4, the exposed area of the zircaloy matrix due to these cracks is minimal. This observation may suggest the presence of a potential self-healing effect [7].

Conversely, in the specimen with a circumferential strain of 42.4%, the weight gain increased significantly, indicating substantial oxidation of the zircaloy matrix due to coating cracks. These results imply that when the burst strain exceeds 25%, oxidation of the outer wall of Cr-coated cladding should be taken into account in fuel safety regulations and accident analyses.

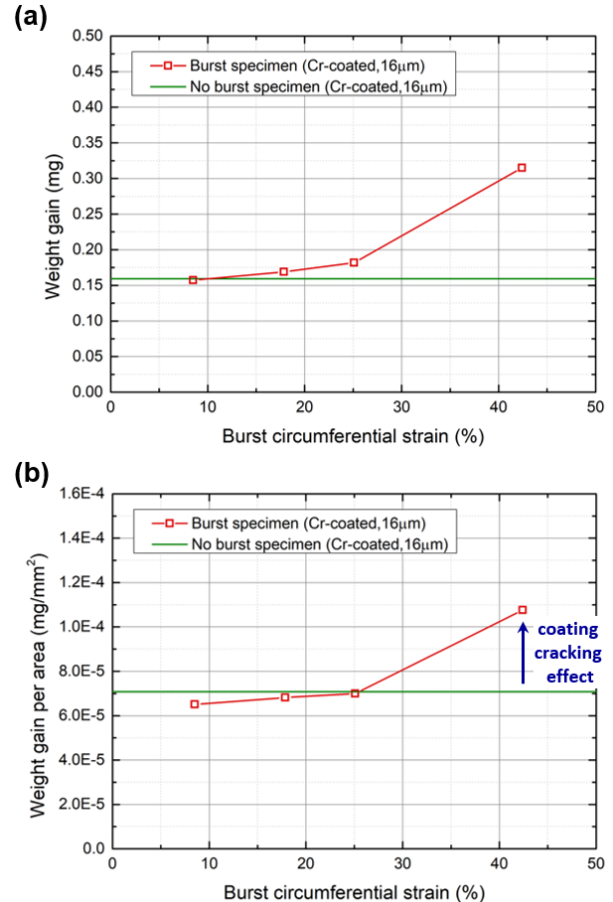


Fig. 7. Oxidation results of burst specimens compared to non-burst specimens (a) weight gain (b) weight gain per area.

#### 4. Conclusions

In this study, observations were made of cladding burst along with corresponding coating cracks, and an analysis was conducted regarding the exposure and oxidation of the Zircaloy matrix resulting from coating cracking. The concentration of coating cracks was noted in the burst area where the circumferential strain was pronounced. It was found that coating cracks do not exert a substantial effect on outer wall oxidation until the circumferential strain reaches 25%. However, beyond this threshold, it is concluded that outer wall oxidation and potential embrittlement may occur in Cr-coated cladding.

#### Acknowledgements

This work was supported by the Nuclear Safety Research Program through the Korea Foundation Of Nuclear Safety(KoFONS) using the financial resource granted by the Nuclear Safety and Security Commission(NSSC) of the Republic of Korea. (No. 00241683)

#### REFERENCES

- [1] Capps, N., et al. (2020). "Integral LOCA fragmentation test on high-burnup fuel." *Nuclear Engineering and Design* 367: 110811.
- [2] Sonnenburg, H., et al. (2016). "Report on fuel fragmentation, relocation and dispersal." Nuclear Energy Agency/Committee on Safety of Nuclear Installations.
- [3] Yook, H., Shirvan, K., Phillips, B., & Lee, Y. (2022). Post-LOCA ductility of Cr-coated cladding and its embrittlement limit. *Journal of Nuclear Materials*, 558, 153354.
- [4] Yook, H., et al. " Integral LOCA experiment to study FFRD phenomena of high burnup ATF clad fuels." Korean Nuclear Society Spring Meeting. 2023.
- [5] Joung, S., Kim, J., Ševeček, M., Stuckert, J., & Lee, Y. (2024). Post-quench ductility limits of coated ATF with various zirconium-based alloys and coating designs. *Journal of Nuclear Materials*, 154915.
- [6] Chung, H. and T. Kassner (1978). Deformation characteristics of Zircaloy cladding in vacuum and steam under transient-heating conditions: summary report.[PWR; BWR], Argonne National Lab., IL (USA).
- [7] Ma, H. B., Zhao, Y. H., Liu, Y., Zhu, J. T., Yan, J., Liu, T., ... & Yao, M. Y. (2022). Self-healing behavior of Cr-coated Zr alloy cladding in high temperature steam oxidation process. *Journal of Nuclear Materials*, 558, 153327.